



Cite this: *Green Chem.*, 2023, **25**, 5068

# Techno-economic analysis and life cycle assessment of mixed plastic waste gasification for production of methanol and hydrogen†

Shaik Afzal,<sup>a,b</sup> Avantika Singh,<sup>\*a,b</sup> Scott R. Nicholson,<sup>b,c</sup> Taylor Uekert,<sup>b,d</sup> Jason S. DesVeaux,<sup>a,b</sup> Eric C. D. Tan,<sup>a</sup> Abhijit Dutta,<sup>a</sup> Alberta C. Carpenter,<sup>b,d</sup> Robert M. Baldwin<sup>b</sup> and Gregg T. Beckham<sup>b,c</sup>

Plastic waste management is an area of concern globally, given the accumulation of plastics in landfills and the natural environment. Gasification can convert mixed plastic waste (MPW) to synthesis gas (syngas), a mixture of carbon monoxide (CO) and hydrogen (H<sub>2</sub>), which can be further converted to commodity chemicals. In this work, we present techno-economic analysis (TEA) and life cycle assessment (LCA) for two gasification pathways that produce methanol and hydrogen from MPW feedstock. In particular, we modeled the gasifier as a dual fluidized bed reactor for MPW gasification in a greenfield, standalone facility. Our analysis indicates that the minimum selling price (MSP) of methanol and hydrogen produced by MPW gasification is \$0.70 kg<sup>-1</sup> and \$3.41 kg<sup>-1</sup>, respectively. For comparison, we also evaluate the production of methanol and hydrogen from municipal solid waste. For MPW gasification processes, the syngas yield (kg syngas per kg plastic) and waste plastic feedstock price have the largest impact on MSP. Waste plastic feedstock prices of <\$0.02 kg<sup>-1</sup> can enable MPW-based processes to achieve cost parity with existing fossil-fuel-derived pathways. Additionally, LCA indicates that methanol and hydrogen produced from MPW gasification can reduce the total supply chain energy use by 52% and 56% respectively when compared with fossil-fuel-derived pathways. However, the greenhouse gas emissions (GHG) from MPW-gasification pathways are estimated to increase by 166% and 36% for methanol and hydrogen, respectively, compared to their current production pathways. Due to the co-product credit of steam and electricity export, MPW gasification pathways have lower levels of smog formation, acidification, non-carcinogenics, ozone depletion, eutrophication and particulates than the respective incumbent processes. Since waste streams are the feedstocks in this study, no energy burden was assigned to the upstream processes. Overall, this work identifies syngas yield and waste plastic feedstock price as the two critical variables with the largest impact on the MSP of products produced by MPW gasification. The outcomes of this work can help guide future research in MPW gasification.

Received 26th February 2023,  
Accepted 25th May 2023

DOI: 10.1039/d3gc00679d

[rsc.li/greenchem](https://rsc.li/greenchem)

## Introduction

Many new technologies are emerging to deal with mixed plastic waste (MPW), including thermal approaches such as

pyrolysis and gasification that use MPW as feedstock to produce new products.<sup>1–12</sup> Gasification, which is the focus of the current study, refers to the partial combustion of carbonaceous feedstocks at temperatures ≥750 °C to produce synthesis gas, or syngas [a mixture of carbon monoxide (CO) and hydrogen (H<sub>2</sub>)].<sup>13</sup> Syngas is a versatile intermediate that can either be used as a feedstock to produce petrochemicals<sup>14</sup> or combusted for power generation.<sup>15,16</sup> Today, steam reforming of natural gas to produce syngas followed by downstream processing is the primary pathway for the production of hydrogen and methanol.<sup>14</sup> Similarly, gasification of municipal solid waste (MSW) can be used to produce syngas that is combusted to generate steam that drives a turbine to produce electricity.<sup>16–18</sup> The syngas can also be processed to produce chemicals like methanol.<sup>19</sup>

<sup>a</sup>Catalytic Carbon Transformation and Scale-Up Center, National Renewable Energy Laboratory, Golden, CO, 80401 USA. E-mail: [gregg.beckham@nrel.gov](mailto:gregg.beckham@nrel.gov), [avantika.nrel@outlook.com](mailto:avantika.nrel@outlook.com)

<sup>b</sup>BOTTLE Consortium, Golden, CO, 80401 USA

<sup>c</sup>Renewable Resources and Enabling Sciences Center, National Renewable Energy Laboratory, Golden, CO, 80401 USA

<sup>d</sup>Strategic Energy Analysis Center, National Renewable Energy Laboratory, Golden, CO, 80401 USA

†Electronic supplementary information (ESI) available: Gasification|mixed plastic waste|methanol|hydrogen|TEA|LCA|municipal solid waste. See DOI: <https://doi.org/10.1039/d3gc00679d>



The selection of oxidant [air, pure oxygen (O<sub>2</sub>), or steam] for gasification depends on the syngas use – either for chemical synthesis or energy generation.<sup>20</sup> Air gasification is typically used for energy generation.<sup>15</sup> In this case, the presence of nitrogen (N<sub>2</sub>) reduces the calorific value of the syngas,<sup>21</sup> but also avoids the capital expenditure (CAPEX) related to air separation. Pure oxygen gasification is also used to produce high calorific value syngas.<sup>22</sup> For syngas used in chemical syntheses, pure O<sub>2</sub> gasification is typically employed to avoid N<sub>2</sub> in the syngas.<sup>21</sup> Additionally, for chemical syntheses that require a molar ratio of H<sub>2</sub>/CO ≥ 2, steam gasification is the preferred pathway, as steam drives steam reforming reactions enhancing the hydrogen content in the syngas.

The motivation to use gasification as a pathway to process MPW is twofold. First, it provides an opportunity to convert unsorted MPW to fuels and valuable chemicals. Second, producing syngas from a waste plastic feedstock can reduce the consumption of natural gas that would have otherwise been used to synthesize the same product. For waste plastic feedstocks specifically, gasification provides a potential added advantage of being “feedstock-agnostic.” For many pathways under consideration in the chemical recycling of plastics, the chemistry of the polymer backbone (C–C, C–O) often dictates the appropriate deconstruction approach.<sup>9</sup> However, for gasification, the composition of plastic waste is not as critical because all C–C and C–O backbone polymers will be converted to CO and H<sub>2</sub>. Due to the high temperature of the gasification reaction and the presence of an oxidant (steam and/or O<sub>2</sub>), the main product of waste plastic gasification is a gaseous stream consisting of CO, H<sub>2</sub>, carbon dioxide (CO<sub>2</sub>), methane (CH<sub>4</sub>), and some higher hydrocarbons. However, in contrast to natural gas and coal gasification, which are mature commercial technologies, waste plastic gasification has been reported to our knowledge only at laboratory and pilot scales.<sup>20</sup>

Most literature reports on waste plastic gasification routes are experimental in nature and limited to the gasifier operation. Lopez *et al.*<sup>20</sup> provided an extensive overview of studies on different gasification types for MPW, emphasizing that the choice of gasifying agent alters the syngas yield and composition. More recently, Midilli *et al.* reviewed investigations into the conversion of waste plastics to hydrogen and discussed results with fluidized bed gasifiers at laboratory and pilot scales (0.04–31.4 kg h<sup>−1</sup> plastic feed rates and ~850 °C).<sup>23</sup> Techno-economic analysis (TEA) of gasification processes has been reported in the literature for biomass<sup>24</sup> and MSW<sup>25</sup> feedstocks. In most studies to date where waste plastics are considered for gasification, MPW is blended with other feedstocks. For instance, Goyal presented a TEA of a 50/50 feed stream of biomass and waste plastics to produce methanol.<sup>26</sup> Systematic and consistent TEA studies exclusively for waste plastic gasification are necessary to understand the economic viability of the gasification pathway using waste plastics as the feedstock.<sup>27</sup>

In this work, we constructed a detailed process model of the gasification pathways for MPW feedstock to produce methanol and hydrogen and conducted a TEA and life cycle

assessment (LCA). We considered MSW as a separate case study to compare technical process performance metrics and economic target metrics against MPW for identical chemical product syntheses. Conceptual process designs were formulated in Aspen Plus, which were then used to estimate CAPEX, operating expenditures (OPEX), and the minimum selling price (MSP) of the corresponding methanol and hydrogen products for each pathway. We also performed a sensitivity analysis on key process variables to highlight opportunities to enhance the economic viability of these pathways. The results from this study identified the factors that can enable chemical synthesis pathways from both MPW and MSW gasification to potentially become economically viable. Furthermore, we used LCA analysis to understand the GHG emissions, supply chain energy requirements, and various other impact metrics for the processes and compared them with fossil-fuel counterparts.

### Gasification feedstocks and pathways

This work aims to study the potential of MPW and MSW as gasification feedstocks to produce methanol and hydrogen. Methanol and hydrogen were chosen as products for the pathways to be studied here as they are important chemicals that involve syngas as an intermediate. With a global production of 110 million metric tonnes per year (MMT per year),<sup>28</sup> methanol is an important petrochemical intermediate. The annual global production of hydrogen is 70 MMT, resulting in annual CO<sub>2</sub> emissions of 830 MMT.<sup>29</sup> Hydrogen from waste is a relatively new area of research motivated by the vision for the hydrogen economy.<sup>30,31</sup> The pathways are hereafter denoted by Feedstock-Product (*e.g.*, MPW-methanol).

An overview of the four pathways presented in this work is provided in Table 1. The experimental data describing reaction temperature, syngas yield, composition, *etc.*, for the respective pathways are taken from the literature.<sup>32,33</sup> Recent plants in planning or construction phases utilizing MPW and MSW as feed have capacities ranging from 120 to 300 metric tonnes per day (MT per D).<sup>19,34</sup> Hence, a feed capacity of 240 MT per D was chosen for all base cases in this study. For context, this capacity represents 7.6% of the total high-density polyethylene (HDPE) and polypropylene (PP) recycled in the United States in 2019.<sup>35</sup> The plant capacity was later varied in the sensitivity analysis to study its impact on the process economics.

**Table 1** Process pathway details. For the MPW feedstock, only steam gasification is used, and hence an indirect gasification design is selected. For MSW feedstock, steam and oxygen are used as oxidants; the combustion reactions provide the energy for gasification, and consequently, a direct gasification design is selected

| Pathway name | Feedstock | Oxidant for gasification | Downstream process | Final product |
|--------------|-----------|--------------------------|--------------------|---------------|
| MPW-methanol | MPW       | Steam                    | Methanol synthesis | Methanol      |
| MPW-hydrogen | MPW       | Steam                    | Water-gas-shift    | Hydrogen      |
| MSW-methanol | MSW       | Steam + oxygen           | Methanol synthesis | Methanol      |
| MSW-hydrogen | MSW       | Steam + oxygen           | Water-gas-shift    | Hydrogen      |



Table 2 lists the ultimate analysis/characteristics of the MPW and MSW assumed in our models. A 50/50 mix of polyethylene (PE) and PP was chosen to represent MPW because of its similarity to the compositions reported in the literature.<sup>36</sup> The carbon and hydrogen weight percentages for MPW reaffirm that the feedstock is close to the stoichiometric monomer unit ( $-\text{CH}_2-$ ) of the polymer backbone of PE and PP, which has 85.7% C and 14.3% H. More than 70% of the waste plastic landfilled in 2019 in the United States has the same chemical composition of carbon and hydrogen weight percentages, which is the important variable for gasification.<sup>35</sup> If the waste plastics contains PET, the chemical composition will also contain oxygen of about 2 wt%.<sup>37</sup> The lower calorific value (LCV) of  $43.4 \text{ MJ kg}^{-1}$  was used as the heat of combustion input parameter needed to characterize the MPW in the Aspen Plus model.<sup>27</sup>

Based on the prices for baled natural HDPE, and post-consumer PP reported by Recycling Markets,<sup>38</sup> a base case price of  $\$0.60 \text{ kg}^{-1}$  was used for the MPW feedstock. Both of these plastics can be mechanically recycled; hence, we varied the feedstock price in the sensitivity analysis to consider alternate polyolefin mixed streams that are not currently recycled and may potentially be available at a lower price (*vide infra*, *Methanol synthesis cases*). The relation between MPW quality and syngas yield is discussed with Table S1.†

The MSW feedstock composition shown in Table 2 was taken from patent literature<sup>33</sup> and is in line with the average MSW composition aggregated from various sources<sup>39</sup> (C-38.8%, H-7.4%, O-37.1%, Ash-14.5%). The feed to the MSW gasifier is assumed to be refuse-derived fuel (RDF). RDF is MSW in pelletized form (2–5 cm) after the removal of glass and metals.

The LCV of MSW used in the model is  $22.7 \text{ MJ kg}^{-1}$ , which is in the range of  $20.8$ – $25.3 \text{ MJ kg}^{-1}$  in the literature for RDF.<sup>40,41</sup> As shown in Table 2, MPW and MSW differ in carbon and oxygen content. The feedstock composition affects the process design of the gasification pathway for that particular feedstock. In MPW steam gasification, due to the lower oxygen content in the waste plastic feedstock, the  $\text{CO}_2$  concentration in the syngas<sup>32</sup> is approximately 5%, and therefore, a  $\text{CO}_2$  removal section is not necessary. Conversely, the  $\text{CO}_2$  concentration in MSW-derived syngas<sup>33</sup> can be as high as 30%–40% due to higher oxygen content in the MSW feedstock (25%–40%). This necessitates an additional  $\text{CO}_2$  removal step before the syngas can be upgraded to chemicals.<sup>33,42</sup>

Hydrogen is a valuable component of the solid feedstock. Hydrogen is high in MPW feedstocks (14%) but low in MSW feedstocks (3%–8%). Similarly, the ash content is much higher in MSW (>15%). The ash produced has to be disposed of in a landfill and therefore incurs an additional disposal cost, assumed here at  $\$59 \text{ per MT}$  as a tipping fee.<sup>43</sup>

As described in the Introduction, the choice of oxidant for a feedstock depends on the target  $\text{H}_2/\text{CO}$  ratio of the syngas, and this choice also impacts the gasifier design. Here, we selected steam for MPW gasification because methanol and hydrogen are the desired products, and steam gasification enables syngas with a high  $\text{H}_2/\text{CO}$  ratio ( $\geq 2$ ) due to reaction stoichiometry. Steam gasification is an endothermic process, and energy must be supplied to drive the reactions; hence an indirect gasification design was used. Conversely, for MSW gasification, steam and oxygen were used as the oxidants. Part of the carbon is converted to  $\text{CO}_2$  in the gasifier and the energy released provides the necessary enthalpy for gasification reactions to proceed; consequently, a direct gasification design was used for the MSW feedstock.

### Methanol production processes

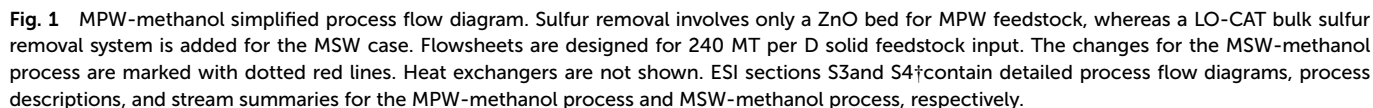
**Process design and modeling assumptions.** The MPW-methanol process flow diagram (PFD) is shown in Fig. 1. MPW in the form of solid granulates with 5 mm nominal particle size<sup>44</sup> is fed into the gasification reactor by screw conveyors, and low-pressure steam is fed from the bottom. MPW gasification uses 480 MT per D of low-pressure steam (steam per MPW = 2) in an indirectly heated gasifier design. The syngas composition at the gasifier outlet is based on an experimental study on steam gasification of PE and PP.<sup>32</sup> The syngas from steam gasification ( $\text{H}_2/\text{CO} \geq 2$ ) is suitable for the methanol synthesis process. Natural gas, purge gas from the recycle loop, and light end vapors from the distillation column are combusted in the combustion reactor to provide supplemental heat. An indirect gasifier that consists of a circulating fluidized bed with olivine as the bed material was assumed in the base design.<sup>45,46</sup> Hot olivine from the combustion reactor provides the heat to the gasification reactor in this indirect gasification process. The mass balance around the gasifier is shown in Table S1.† The syngas leaves from the top of the gasification reactor. The dry syngas yield (amount of syngas produced per kg of solid input) from steam gasification is  $2.1 \text{ Nm}^3 \text{ kg}^{-1}$  MPW, or  $1.4 \text{ kg kg}^{-1}$  MPW.<sup>32</sup> Post gasification, the tar reformer is deployed to decrease hydrocarbon content by reforming to produce  $\text{H}_2$  and CO. The conversion data for the tar reformer are taken from Phillips *et al.*<sup>45</sup> Consequently, in our model, the mass flow rate of ( $\text{H}_2 + \text{CO}$ ) in the product stream increases from 159.1 MT per D to 306.3 MT per D. Tar reforming is essential as the tar compounds condense at lower temperatures in downstream equipment, causing flow problems. A particulate removal system that includes cyclones and an electrostatic precipitator is used to clean the syngas.

Next, the syngas is cooled to remove unreacted water and is compressed to 3 bar. Hydrogen sulfide ( $\text{H}_2\text{S}$ ) is removed in a zinc oxide ( $\text{ZnO}$ ) fixed-bed reactor. After that, methane-rich

**Table 2** Feed characterization for MPW<sup>32</sup> and MSW (wet basis, % by wt)

| Parameter                               | MPW    | MSW  |
|---|--------|------|
| Carbon, C                               | 85.9   | 44.3 |
| Hydrogen, H                             | 14.0   | 6.9  |
| Nitrogen, N                             | 0.1    | 0.5  |
| Sulfur, S                               | <0.005 | 0.3  |
| Oxygen, O                               | <0.01  | 28.9 |
| Ash                                     | <0.1   | 18.3 |
| Heat of combustion, $\text{MJ kg}^{-1}$ | 43.4   | 22.7 |





The process shown in Fig. 1 was modified for MSW feedstock with the following major changes: 106 MT per D of low-pressure steam (steam per MSW = 0.44) and 50 MT per D of oxygen (oxygen per MSW = 0.21) were used as oxidants in a directly heated gasifier.<sup>33</sup> Unlike indirect gasification for MPW, the direct gasification process for MSW does not have heat input through circulating olivine. Hence, oxygen is added as

**Capital cost and annual operating cost estimation.** The CAPEX and annual OPEX for the MPW-methanol process are shown in Fig. 2. The CAPEX was estimated by correlating with similar equipment from literature reports.<sup>45,46,51</sup> The OPEX data used is shown in Table S2.† Overall, the installed cost is \$75M, and the total capital investment (TCI) for the 240 MT per D MPW-methanol plant is \$149M (Fig. 2A). The methanol section is the major contributor to the plant CAPEX at 49%, mainly due to the four-stage makeup gas compressor and the steam turbine. The gasification and syngas preparation sections, which are the main areas for syngas production, contribute 29% to the CAPEX. A 25% contribution was added for outside battery limit (OSBL) costs. Since gasifiers and feed systems for these non-conventional feedstocks are not common equipment, we understand that there are CAPEX uncertainties associated with these systems. We capture the





**Fig. 2** CAPEX, OPEX, and MSP breakdown for MPW-methanol process. (A) CAPEX contributions for the MPW-methanol process. Feed: 240 MT per D MPW; product: 353 MT per D methanol. The methanol synthesis section includes gas compression to 80 bar and the steam turbine, resulting in the largest contribution to CAPEX. A detailed breakdown of CAPEX by process section is given in Table S3.† (B) OPEX contributions for the MPW-methanol process. BFW-Boiler feedwater, CW-cooling water. The feedstock cost ( $\$0.60 \text{ kg}^{-1}$ ) dominates the OPEX. A detailed breakdown of OPEX for variable and fixed costs is shown in Table S4.† (C) A comparison of MSP for MPW-methanol, MSW-methanol, and natural gas (NG)-based processes. The breakdown and net MSP for MPW-methanol process are shown in separate bars. In the MSW-methanol case, the feedstock cost is zero. A detailed MSP breakdown by process section is given in Table S5.†

impacts of changes in investment costs in our sensitivity analysis.

The annual OPEX is  $\sim \$62\text{M}$ . This cost is mainly driven by the feedstock cost of waste plastic ( $\$0.60 \text{ kg}^{-1}$ ), which represents 70% of the total OPEX (Fig. 2B). The other major operating costs are from electricity use for gas compression (8%), natural gas import as fuel (5%), and catalysts and water requirements (5%). The capital cost and annual operating cost breakdowns for the MSW-methanol process are shown in Fig. S1.† The operating cost reduces to about  $\$11\text{M}$ , with the major contribution (54%) from the fixed variable operating costs, which include labor, supervision, and overhead costs. The operating cost is significantly lower than the MPW-methanol case, since the expensive MPW feed is now replaced with a zero cost RDF feed. The utilization of MSW as a feed comes with the credit of a tipping fee, which is an additional revenue stream for the MSW-methanol plant, and this variable is varied in the sensitivity analysis, as shown in Fig. S4.†

**MSP of the MPW-methanol and MSW-methanol cases.** We performed a discounted cash flow rate of return analysis based on the capital cost and annual operating cost estimations. The MSP was estimated by setting the net present value (NPV) to zero with a 10% internal rate of return (IRR). 60% of the TCI was assumed to be obtained by a loan at an 8% interest rate with a loan term of 10 years. The MPW-methanol process produces 343 MT per D of methanol from 240 MT per D of MPW, resulting in a yield of 1.47 kg methanol per kg MPW. The MSP for methanol derived from MPW steam gasification is estimated to be  $\$0.70 \text{ kg}^{-1}$ , more than twice the price of fossil-fuel-derived methanol at  $\$0.30 \text{ kg}^{-1}$  (2015–19 five-year average from the industry database). The contributions to the MSP are shown in Fig. 2C, and the breakdown by process section is shown in Fig. S2.† The major contributor is the waste plastic feedstock cost, which contributes 58% to the MSP of metha-

nol. The next most significant contributor, capital investment, contributes 24% to the MSP (shown in dark green in Fig. 2C).

For the MSW feedstock case, the MSP of methanol from this process is estimated at  $\$0.55 \text{ kg}^{-1}$ . Despite our assumption of a zero feedstock cost for MSW, the predicted MSP for methanol remains nearly twice that of fossil-fuel-derived methanol. The MSP breakdown by process area is shown in Fig. S3.† The base case simulation for the MSW-methanol process estimates that 112 MT per D of methanol is produced by MSW gasification processing 240 MT per D of MSW. Thus the mass yield is 0.48 kg methanol per kg MSW, which is in good agreement with the yield reported in commercial plants for the MSW to methanol pathway (0.40–0.50 kg methanol per kg MSW).<sup>52,53</sup>

**Sensitivity analysis on key cost drivers for methanol production.** Next, we varied process parameters to assess their impact on the MSP, as shown in Fig. 3. The most important variable that has an impact on MSP is syngas yield. The base case uses a value of 1.4 kg dry syngas per kg MPW based on the experimental results of Wilk and Hofbauer.<sup>32</sup> Reducing the yield to 1.0 kg syngas per kg MPW results in a methanol MSP of  $\$0.91 \text{ kg}^{-1}$ . Syngas yield has a large impact on the MSP of the final product and hence is a key metric to measure the efficiency of gasification in the gasifier. If a portion of the solid MPW feedstock, which is purchased at  $\$0.60 \text{ kg}^{-1}$ , is not converted to syngas in the gasifier, it ends up as solid residue, incurring a disposal fee of  $\$59 \text{ per MT}$  which is the US average landfill tipping fee.<sup>43</sup> Hence, an inefficient gasifier design not only reduces the syngas yield but also results in solid waste residue that incurs a landfilling fee, impacting process economics. The feedstock cost has the next largest impact on the methanol MSP. Specifically, a  $\pm 33\%$  change in the feedstock cost from the base case price of  $\$0.60 \text{ kg}^{-1}$  affects the methanol MSP by up to 20%, changing it from  $\$0.56 \text{ kg}^{-1}$  to  $\$0.83 \text{ kg}^{-1}$ .





**Fig. 3** Sensitivity analysis for the MPW-methanol process. The syngas yield and feedstock cost have the largest impact on MSP. For the syngas yield variable, a yield greater than 1.4 kg dry syngas per kg solid results in a mass balance error for carbon, and hence only a lower point was considered. Theoretically, a much higher yield (2.3 kg dry syngas per kg MPW) is possible through steam gasification if all solid MPW was converted only to (CO + H<sub>2</sub>) without any side products or losses by char formation. But not all carbon atoms end up as CO in the gasifier, which is the main reason for the increase in mass yield. Only about 29% of total carbon input ends in CO. The remaining carbon is in hydrocarbons (CH<sub>4</sub>, C<sub>2</sub>H<sub>4</sub>, C<sub>3</sub>H<sub>8</sub>, and C<sub>10</sub>H<sub>8</sub>) which are reformed later in the tar and steam reformers to increase the (H<sub>2</sub> + CO) content. The gasifier outlet syngas composition is shown in Table S1.† Sensitivity analysis for the MSW-methanol process is shown in Fig. S4.†

The “methanol loop purge fraction” is the fraction of the vapor stream from the knock-out pot that is routed to fuel, as shown in Fig. 1. Since the loss of carbon as fuel results in a drop in carbon efficiency to methanol, the purge fraction variable impacts the methanol MSP. The base case purge fraction is 15%. Changing the purge fraction by  $\pm 10\%$  across the base case results in a  $\pm 10\%$  change in MSP. Further discussion on the selection of the purge fraction variable is included in the ESI, section S3.†

Also, from Fig. 3, “Single pass conversion to methanol” refers to the single-pass conversion of CO and CO<sub>2</sub> in the methanol formation reactions as shown in Table 3 which was fixed at 40% in the base case. To quantify the economic impact of catalyst performance, the single-pass conversion was varied by  $\pm 10\%$ , which results in a  $-7\%$  to  $+10\%$  impact on methanol MSP. Similarly, “Methanol conversion to DME” refers to the conversion of methanol to unwanted side-products consisting of low boiling compounds, modeled as DME here. When varied from 5% to 15%, the methanol side-products impact the MSP by less than 1%. Any side-products formed in the methanol reactor are removed with the light ends of the distillation column and combusted as fuel in the gasifier, thereby reducing the amount of natural gas to be imported. Any loss of methanol product is compensated by a reduction in natural gas import; thus, the impact on overall process economics is minimal.

Increasing plant size has a lower effect on MSP than syngas yield and the MPW feedstock cost. From Fig. 3, doubling the plant capacity to 500 MT per D results in a drop in MSP by only 8%. For the same reasons, changes in TCI also do not have a major impact on methanol MSP. When varied by  $-15\%/+30\%$ , the TCI has an impact of  $-5\%/+8\%$  on the methanol MSP.

The information from the sensitivity analysis can also inform catalyst selection. For instance, the methanol catalyst cost and methanol conversion to DME have a relatively small effect on MSP, whereas single pass conversion to methanol is much more influential. Therefore, choosing a more expensive catalyst to increase the single pass conversion to methanol could be a good strategy to reduce the MSP.

In terms of financial factors, the IRR was set to 10% in the base case. Varying IRR by  $\pm 5\%$  results in a corresponding change in the MSP by  $\pm 8\%$ . The income tax rate in the base case is 21%. This rate has a minimal effect on the MSP; varying it from 15% to 35% only changes the MSP by  $\pm 1\%$ .

### Hydrogen production processes

**Process design and modeling assumptions.** Fig. 4 shows the PFD for the MPW-hydrogen process. In the MPW-hydrogen and MSW-hydrogen processes, the gasification and syngas preparation sections are identical to the methanol processes for the respective feedstocks. After syngas preparation, the



**Table 3** Summary of results for all cases. The lower GHG emissions for MSW-based processes results when credit is considered for the avoidance of landfill methane emissions. The steam integration system with steam sources and sinks are shown in Fig. S11†

| Base-case results   | MPW-methanol                        | MPW-hydrogen          | MSW-methanol                        | MSW-hydrogen          |
|---|-------------------------------------|-----------------------|-------------------------------------|-----------------------|
| <b>Gasification &amp; gas clean-up</b>  |                                     |                       |                                     |                       |
| Feed-rate, MT per D   |                                     |                       | 240                                 |                       |
| LP steam input to gasifier, MT per D  |                                     | 480                   |                                     | 106                   |
| O <sub>2</sub> input to gasifier, MT per D  |                                     | —                     |                                     | 50                    |
| Gasifier temperature, °C  | 835                                 |                       |                                     | 786                   |
| Gasifier pressure, bar  |                                     |                       | 1                                   |                       |
| <b>Raw syngas composition<sup>34</sup> (dry basis), vol %</b>                                     |                                     |                       |                                     |                       |
| N <sub>2</sub>  |                                     | 0                     |                                     | 1                     |
| H <sub>2</sub>  |                                     | 46                    |                                     | 12                    |
| CO  |                                     | 22                    |                                     | 20                    |
| CO <sub>2</sub>   |                                     | 5                     |                                     | 41                    |
| CH <sub>4</sub>   |                                     | 17                    |                                     | 10                    |
| C <sub>2</sub> H <sub>4</sub>   |                                     | 8                     |                                     | 0                     |
| C <sub>2</sub> H <sub>6</sub>   |                                     | 1                     |                                     | 10                    |
| C <sub>3</sub> H <sub>6</sub>   |                                     | 0                     |                                     | 0                     |
| C <sub>3</sub> H <sub>8</sub>   |                                     | 1                     |                                     | 5                     |
| C <sub>10</sub> H <sub>8</sub>  |                                     | 1                     |                                     | 1                     |
| Solid residue from gasifier, MT per D   |                                     | 2                     |                                     | 56.8                  |
| H <sub>2</sub> /CO ratio in gasifier outlet   |                                     | 2.1                   |                                     | 0.6                   |
| Tar reformer temperature, °C  |                                     |                       | 890.0                               |                       |
| Tar reformer furnace duty, Gcal h <sup>-1</sup>   |                                     | 7.9                   |                                     | 6.1                   |
| <b>Tar reformer performance, % conversion to CO and H<sub>2</sub><sup>45</sup></b>                |                                     |                       |                                     |                       |
| Methane (CH <sub>4</sub> )  |                                     |                       | 20                                  |                       |
| Ethane (C <sub>2</sub> H <sub>6</sub> )   |                                     |                       | 90                                  |                       |
| Ethylene (C <sub>2</sub> H <sub>4</sub> )   |                                     |                       | 50                                  |                       |
| Tars (C <sub>10+</sub> )  |                                     |                       | 95                                  |                       |
| Benzene (C <sub>6</sub> H <sub>6</sub> )  |                                     |                       | 70                                  |                       |
| Steam condensate after tar reformer, MT per D   | 222.5                               | 222.5                 | 32.5                                | 32.5                  |
| Raw syngas, after particulate removal, MT per D   | 472.1                               | 472.1                 | 306.4                               | 306.4                 |
| External natural gas used in combustion section (MPW)/reformer furnace (MSW), MT per D            | 25.2                                | 44.8                  | 8.1                                 | 14.9                  |
| HRSG-1 duty (hot fluid: flue-gas), Gcal h <sup>-1</sup>   | 18.6                                | 27.1                  | 3.6                                 | 4.5                   |
| HRSG-2 duty (hot fluid: tar reformer outlet), Gcal h <sup>-1</sup>                                | 20.5                                | 20.5                  | 6.5                                 | 6.5                   |
| HRSG-3 duty (hot fluid: SMR outlet), Gcal h <sup>-1</sup>   | 31                                  | 31                    | 7.7                                 | 17.5                  |
| Medium pressure steam (45 bar) input to turbine, MT per D   | 2199                                | 2468.5                | 560.1                               | 895.2                 |
| Turbine electricity production, kW  | 9205.5                              | 12 210                | 2769.8                              | 4427.8                |
| <b>Syngas preparation</b>   |                                     |                       |                                     |                       |
| Compressor duty, kW   | 1976.7                              | 1976.7                | 907.8                               | 907.8                 |
| Low pressure steam (3 bar) input to SMR, MT per D   | 795.3                               | 795.3                 | 174.1                               | 426.9                 |
| Steam methane reformer furnace duty, Gcal h <sup>-1</sup>   | 19.7                                | 17.6                  | 3.7                                 | 6.7                   |
| Steam condensate after SMR, MT per D  | 611.9                               | 611.9                 | 155.5                               | 380.5                 |
| Syngas feed to methanol synthesis/water-gas-shift, MT per D                                       | 655.6                               | 655.6                 | 324.8                               | 352.7                 |
| <b>Main reaction in SMR: CH<sub>4</sub> + H<sub>2</sub>O → CO + 3H<sub>2</sub></b>                |                                     |                       |                                     |                       |
| <b>Methanol synthesis loop/water-gas-shift</b>  |                                     |                       |                                     |                       |
| Main syngas compressor duty, kW   | 11 870.6                            | 6087.3                | 4132.2                              | 2273.0                |
| Fresh feed to methanol synthesis loop, MT per D   | 655.6                               | —                     | 203.8                               | —                     |
| Recycle flow, MT per D  | 680.8                               | —                     | 222.8                               | —                     |
| Purge stream flowrate used as fuel in combustion section, MT per D                                | 120.1                               | —                     | 39.3                                | —                     |
| <b>Reactions in methanol synthesis reactor<sup>48</sup></b>                                       |                                     |                       |                                     |                       |
| CO + 2H <sub>2</sub> → CH <sub>3</sub> OH   | X <sub>CO</sub> = 0.4               | —                     | X <sub>CO</sub> = 0.4               | —                     |
| CO <sub>2</sub> + 3H <sub>2</sub> → CH <sub>3</sub> OH + H <sub>2</sub> O                         | X <sub>CO<sub>2</sub></sub> = 0.4   | —                     | X <sub>CO<sub>2</sub></sub> = 0.4   | —                     |
| 2CH <sub>3</sub> OH → CH <sub>3</sub> – O – CH <sub>3</sub> + H <sub>2</sub> O                    | X <sub>CH<sub>3</sub>OH</sub> = 0.1 | —                     | X <sub>CH<sub>3</sub>OH</sub> = 0.1 | —                     |
| <b>Reactions in water-gas-shift reactor</b>   |                                     |                       |                                     |                       |
| H <sub>2</sub> O + CO → CO <sub>2</sub> + H <sub>2</sub>  | —                                   | X <sub>CO</sub> = 0.9 | —                                   | X <sub>CO</sub> = 0.9 |
| <b>Methanol distillation/pressure swing adsorption</b>  |                                     |                       |                                     |                       |
| Methanol distillation column 1 top stage pressure, bar  | 9                                   | —                     | 9                                   | —                     |
| Methanol distillation column 1 feed temperature, °C   | 71                                  | —                     | 71                                  | —                     |
| Light ends column vapor used as fuel in combustion section (MPW)/reformer furnace (MSW), MT per D | 34.6                                | —                     | 16.1                                | —                     |
| Methanol distillation column 2 top stage pressure, bar  | 1                                   | —                     | 1                                   | —                     |
| Methanol distillation column 2 feed temperature, °C   | 101                                 | —                     | 101                                 | —                     |
| PSA off-gases used as fuel in combustion section (MPW)/reformer furnace (MSW), MT per D           | —                                   | 692.9                 | —                                   | 135.2                 |
| Final product flowrate (methanol/hydrogen), MT per D  | 353.8                               | 69.8                  | 114.5                               | 22.6                  |
| <b>Overall process performance</b>  |                                     |                       |                                     |                       |
| MSP, \$ kg <sup>-1</sup>  | 0.70                                | 3.41                  | 0.55                                | 3.24                  |
| CO <sub>2</sub> emissions, kg CO <sub>2</sub> per kg product                                      | 1.1                                 | 12.8                  | 1.7, -0.9                           | 15.6, 2.6             |
| Product yield, kg product per kg solid feedstock  | 1.47                                | 0.29                  | 0.48                                | 0.09                  |
| Total capital investment (TCI), \$M   | 149                                 | 145                   | 79                                  | 93                    |
| Annual operating cost, \$M  | 62                                  | 60                    | 11                                  | 12                    |





**Fig. 4** MPW-hydrogen process flow diagram. This process flow diagram is identical to the MPW-methanol process in the gasification and syngas preparation sections. After gas compression, a fixed bed reactor is used for the water–gas-shift reaction. The changes for the MSW-hydrogen process relative to the MPW-hydrogen process are marked in red. ESI sections S5 and S6† contain the detailed process flow diagrams and the stream summaries for the MPW-hydrogen and the MSW-hydrogen processes, respectively.

syngas is compressed to 20 bar and fed to a water–gas-shift (WGS) reactor operating at 20 bar and 345 °C. The single-pass conversion was set to 90%,<sup>54</sup> and hence a recycle loop was not employed. The syngas from the WGS section is cooled to 32 °C and then passed through a pressure swing adsorption (PSA) unit. The PSA unit consists of a series of fixed beds with adsorbents that adsorb the impurities, primarily CO<sub>2</sub>, CO, H<sub>2</sub>O, and N<sub>2</sub>. The PSA unit produces two streams: 99.9% pure H<sub>2</sub> at 20 bar and an off-gases stream at 2 bar. The off-gases contain CO and H<sub>2</sub>, which are routed to the reformer as fuel.<sup>55</sup>

The mass yield for the MPW-hydrogen process from our model is 0.29 kg H<sub>2</sub> per kg MPW. MPW-to-hydrogen processes in the literature report H<sub>2</sub> production rates of 0.30–0.40 kg kg<sup>−1</sup> MPW.<sup>20</sup> Experimental studies in the literature investigating plastic waste-to-hydrogen use pyrolysis followed by steam reforming.<sup>20,56</sup> The plastic waste is converted into long-chain hydrocarbons, and the hydrocarbons are reformed in a typical steam reformer to produce H<sub>2</sub> and CO. A reactor is then used to enhance hydrogen production *via* WGS, as shown in Table 3. The alternative pathway to produce hydrogen from plastic waste is steam gasification, followed by steam reforming. Lopez *et al.*<sup>57</sup> studied steam gasification of HDPE followed

by steam reforming and reported a hydrogen yield of 0.36 kg H<sub>2</sub> per kg HDPE. Because this work focuses on the gasification route through syngas, the latter pathway, *i.e.*, steam gasification plus steam reforming, has been considered in this study.

**Capital cost and annual operating cost estimation.** The capital cost and annual operating cost breakdown for the MPW-Hydrogen process are shown in Fig. 5. The installed cost for the MPW-hydrogen plant processing 240 MT per D of MPW is \$73M, and the corresponding TCI is \$145M. The water–gas-shift section contributes 37% to the CAPEX dominated by the compressor cost. The gasification and syngas preparation sections together contribute 31% to the CAPEX. The annual OPEX is \$60M, of which 72% is contributed by the feedstock cost (\$0.60 kg<sup>−1</sup>). The fixed costs contribute 13% to the OPEX, and the natural gas import for furnace duty contributes 7%. The CAPEX and annual OPEX breakdowns for the MSW-hydrogen process are shown in Fig. S5.† Similar to the methanol case described earlier, the MSW-hydrogen process has a much lower OPEX of \$12M, mainly due to avoidance of the expensive MPW feedstock.

**MSP of the MPW-hydrogen case.** The hydrogen MSP for the MPW-hydrogen process is estimated to be \$3.41 kg<sup>−1</sup>. The MSP







**Fig. 5** CAPEX, OPEX, and MSP breakdown for MPW-hydrogen process (MPW: 240 MT per D feedstock, 70 MT per D hydrogen). (A) Detailed breakdown of CAPEX by process section is given in Table S12.† (B) A detailed breakdown of OPEX for variable and fixed costs is given in Table S13.† (C) A comparison of MSP for MPW-Hydrogen, MSW-hydrogen, and natural gas (NG)-based processes. The breakdown and net MSP for the MPW-hydrogen process are shown in separate bars. In the MSW-hydrogen case, the feedstock cost is zero. A detailed MSP breakdown by process section is given in Table S14.†

breakdown for hydrogen by MPW gasification is shown in Fig. 5C, and the breakdown by process area is given in Fig. S6.† The main driver of MSP is the feedstock cost of waste plastic, which is assumed to be  $\$0.60 \text{ kg}^{-1}$  in the base case and contributes roughly 61% to the hydrogen MSP. The hydrogen MSP from the MPW gasification process is almost three times that of fossil-fuel hydrogen (2015–19 five-year average from industry database), which is  $\$1.15 \text{ kg}^{-1}$ . The reason for this large difference can be attributed to the difference in the feedstock costs ( $\$0.60 \text{ kg}^{-1}$  for MPW compared to  $\$0.15 \text{ kg}^{-1}$  for natural gas). The second reason is the inherent reaction stoichiometry of the reaction pathway to hydrogen, which is highlighted in the Discussion.

Our TEA analysis predicts a hydrogen MSP of  $\$3.24 \text{ kg}^{-1}$  for the MSW-hydrogen process. A zero feedstock cost was assumed for MSW in the base case. The MSP breakdown by process areas is shown in Fig. S7.†

Comparing MPW-hydrogen and MSW-hydrogen, we observe a similar trend as observed with methanol in Fig. 2. Even though the large feedstock contribution to the MSP is reduced drastically in the MSW case, there is a corresponding increase in CAPEX and other operational costs stemming from additional unit operations in the MSW process ( $\text{CO}_2$  recovery unit) and the lower mass yield of the process.

**Sensitivity analysis on key cost drivers for hydrogen production.** The tornado plot for the sensitivity analysis of the MPW-hydrogen process is shown in Fig. 6. The syngas yield has a major impact on the MSP. Reducing the syngas mass yield to 1 kg dry syngas per kg solid feed increases the hydrogen MSP by 32%. As explained earlier, any reduction in syngas yield incurs a penalty because the solids from the gasifier are assumed to be disposed of at the US average tipping fee of  $\$59$  per MT. Paying for the feedstock and solid residue disposal affects the process economics leading to an increase in the hydrogen MSP.

The feedstock cost has the second highest impact on the MSP. By varying the feedstock cost from  $\$0.40 \text{ kg}^{-1}$  to

$\$0.80 \text{ kg}^{-1}$  (base case feedstock price is  $\$0.60 \text{ kg}^{-1}$ ), the hydrogen MSP changes by  $\pm 20\%$  from the base case. Similar to the methanol case, the hydrogen MSP drops to  $\$1.35 \text{ kg}^{-1}$  at zero feedstock price, approaching the fossil-fuel hydrogen price.

The PSA hydrogen recovery was varied between 60% and 90%, based on information from a PSA technology licensor.<sup>58</sup> The hydrogen MSP changed by +22% and –15%, respectively. The off-gases are combusted as fuel, and diverting the hydrogen to fuel negatively impacts hydrogen MSP.

Furthermore, doubling the plant capacity to 500 MT per D reduces hydrogen MSP by only 8%. The process variables of steam/carbon ratio in the steam reformer and WGS reactor have negligible impacts on MSP. Hence, the steam/carbon ratio should be decided based on the catalyst requirements, which usually range from 2.5 to 5.<sup>55</sup> Varying the WGS reaction conversion from 80% to 100% has only a  $\pm 1\%$  impact on the hydrogen MSP.

**Material flows through industry (MFI) analysis methanol.** The supply chain energy and greenhouse gas (GHG) analysis for the four process pathways was performed with the publicly available online Materials Flows through Industry (MFI) tool.<sup>59</sup> The relevant process stream results from the Aspen Plus models were used as process inventory inputs to MFI. Co-product credits are taken wherever applicable, such as steam and electricity export. For the MPW feedstock, we have included the impacts from curbside recycling collection and sorting at a Material Recovery Facility.<sup>60</sup> For MSW, we have assumed no upstream burden and energy calculations have been included from the plant gate onwards.

The calculated supply chain energy requirements for the MPW-methanol and MSW-methanol cases are shown in Fig. 7A. The supply chain energy requirement for the fossil-fuel-derived methanol is  $37 \text{ MJ kg}^{-1}$ . The major contributor to supply chain energy is the natural gas feedstock, which is absent in the MPW and MSW cases as they are classified as “waste” with no associated upstream burden. Hence, 52% and 73% of supply chain energy reductions are estimated for the



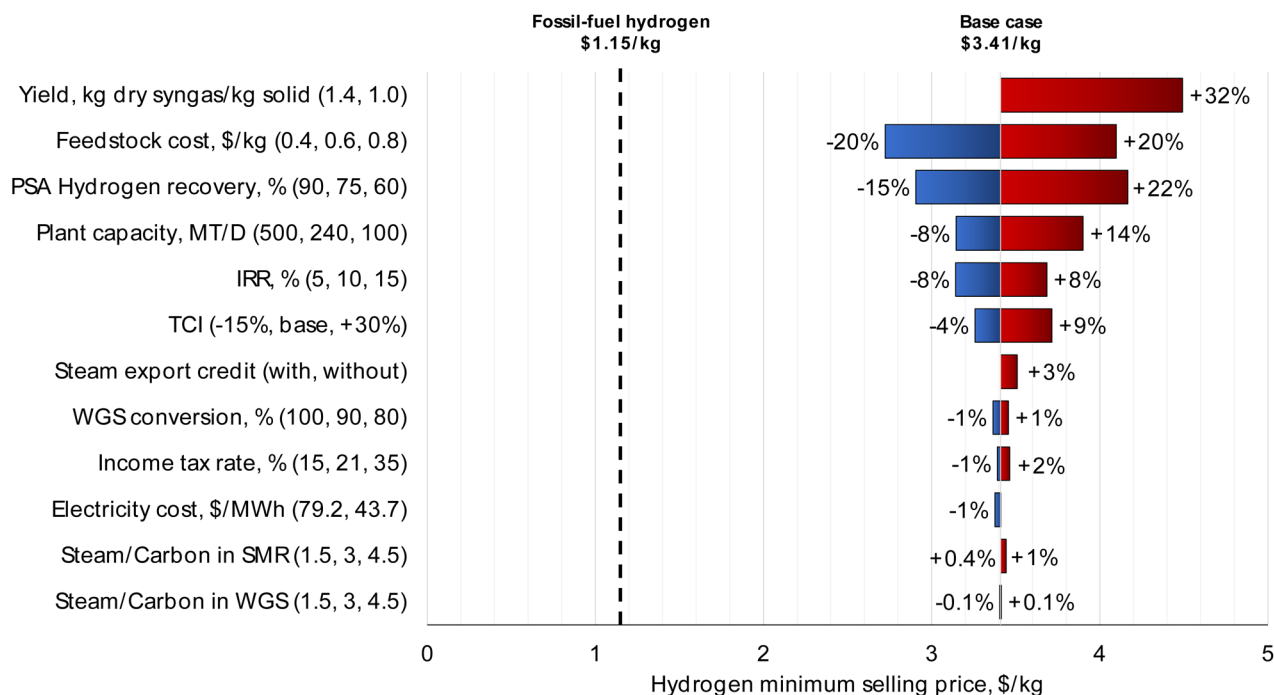


**Fig. 6** Sensitivity analysis for the MPW-hydrogen process. The largest impact on MSP is from syngas yield (kg dry syngas per kg solid feedstock) and waste plastic feedstock cost (\$0.60 kg<sup>-1</sup>). Discussion on syngas yield is included in the caption of Fig. 3. Sensitivity analysis for the MSW-hydrogen process is shown in Fig. S8†

MPW-methanol and MSW-methanol cases relative to conventional methanol production, respectively.

The supply chain GHG emissions for the methanol processes are shown in Fig. 7B. The fossil-fuel-derived methanol supply chain GHG emissions are estimated by MFI at 0.4 kg CO<sub>2</sub> equivalent (CO<sub>2</sub>e) per kilogram of methanol. The major contributor to the GHG emissions of the fossil-fuel-derived methanol is the fuel used in the steam methane reformer furnace. For the MPW-methanol process, the supply chain GHG emissions are 1.1 kg CO<sub>2</sub>e per kg methanol, an increase of 166% from the fossil-fuel methanol. This rise in GHG emissions is due to the increased energy demand in the syngas production unit for the MPW-methanol process. In a typical natural gas-based methanol plant, only a single reformer is used to produce the syngas,<sup>61</sup> whereas for the MPW feedstock, the reforming and gasification reactions occur in three unit operations, namely in the gasification reactor, tar reformer, and steam reformer (Fig. 1). All three reactors involve endothermic reactions that require fuel to run the reactors, resulting in increased energy demand (Table 3). Other configurations with variations in gas conditioning operations, different heat integration, and diverting more process gases (at the expense of lower product yields) instead of using fossil fuel, could lower the GHG emissions.<sup>62,63</sup>

The GHG emissions for the MSW-methanol process are 1.7 kg CO<sub>2</sub>e per kg methanol, almost four times that of the fossil-fuel-derived methanol (0.4 kg CO<sub>2</sub>e per kg methanol). As noted earlier, the low syngas yield of the MSW-methanol results in increased energy demand per kg of methanol. The

carbon efficiency of the MSW-methanol process is only 38%, as illustrated in Fig. S9† when compared to 63% in the MPW-methanol case (Fig. S10†). Almost 33% of the carbon in MSW is lost as CO<sub>2</sub>. However, the usage of MSW as a gasification feedstock avoids methane and CO<sub>2</sub> emissions that would otherwise have been emitted at a landfill; hence, a CO<sub>2</sub> credit can be claimed for the MSW case. Taking the credit into account (1.6 kg CO<sub>2</sub>e avoided per kg MSW),<sup>64</sup> the overall CO<sub>2</sub> emissions become negative and are estimated to be -0.9 kg CO<sub>2</sub>e per kg methanol. Methane has almost 25 times the global warming potential (GWP)<sup>65</sup> of CO<sub>2</sub>, and hence avoidance of the methane emissions results in the sizable CO<sub>2</sub> credit for the MSW-methanol process. Some landfills have facilities to capture landfill gas and generate electricity, and the credit in those scenarios is lower. For instance, at 75% landfill gas collection efficiency and flaring of the gas, the credit would be 0.4 kg CO<sub>2</sub>e avoided per kg MSW.<sup>66</sup>

We have not assumed any such CO<sub>2</sub> credit for the MPW waste because the inorganic carbon in waste plastics does not decompose anaerobically at an appreciable rate.<sup>67</sup> A recent study by Royer *et al.*<sup>68</sup> showed that when exposed to sunlight, waste polyethylene emitted methane, but the emission rates were low (9.3 × 10<sup>-8</sup> kg CO<sub>2</sub>e per kg plastic per day). Additionally, sunlight does not reach all the plastic in a landfill, so this contribution would likely be negligible.

**Hydrogen.** The supply chain energy requirements for the hydrogen processes are shown in Fig. 7C. Compared to fossil-fuel hydrogen, the MPW-hydrogen and MSW-hydrogen cases are predicted to exhibit lower supply chain energy require-



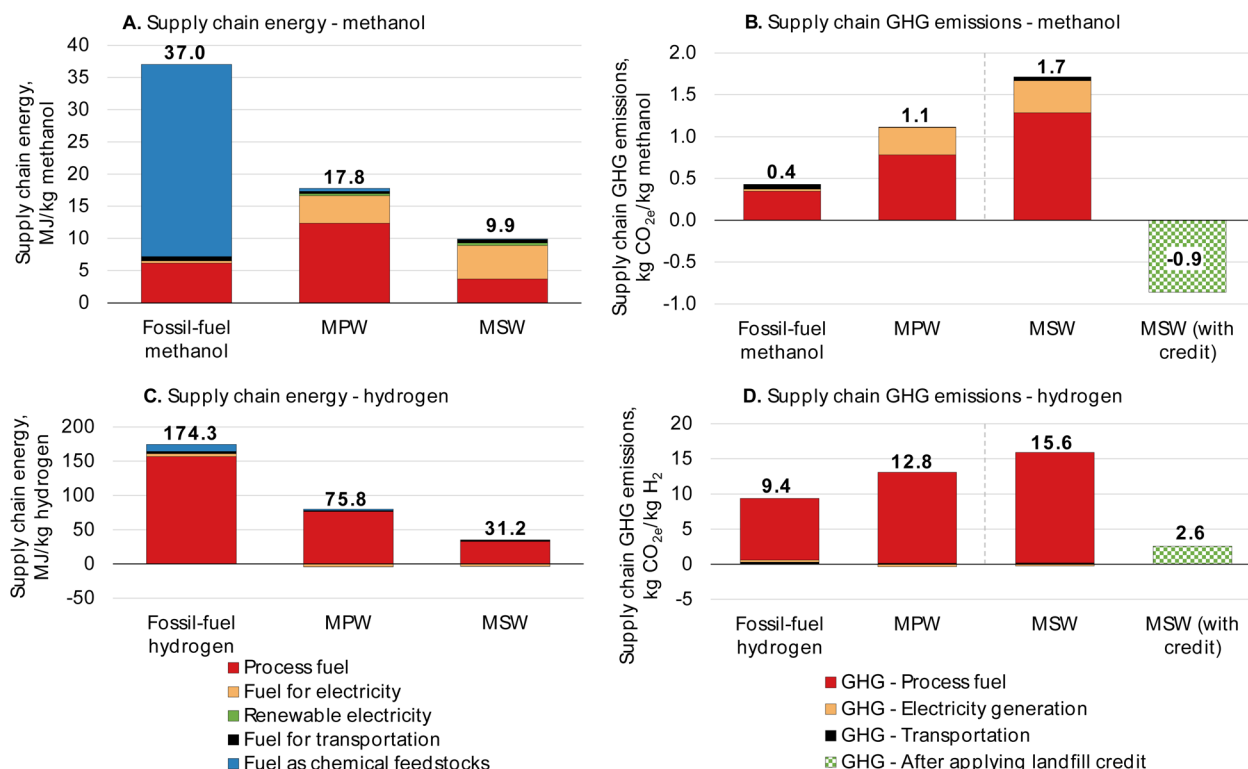


**Fig. 7** Materials Flows through Industry supply chain results for the process configurations presented for all four cases in this analysis. Supply chain energy requirements decrease for MPW- and MSW-based processes because feedstock is considered “waste” without any inherent energy. GHG emissions for all MPW cases increase from fossil-fuel counterparts. The credit for MSW is due to the avoidance of CO<sub>2</sub> emissions at the landfill. All results from the MFI analysis are given in Tables S18 and 19.†

ments with reductions of 56% and 82%, respectively. The fossil-fuel hydrogen case considers natural gas as feedstock, and this feedstock energy increases the overall supply chain energy requirements for the fossil-fuel hydrogen case compared to the MPW and MSW cases.

The supply chain GHG emissions for the hydrogen processes are shown in Fig. 7D. Hydrogen production from natural gas is estimated to exhibit GHG emissions of 9.4 kg CO<sub>2e</sub> per kg hydrogen. For the MPW-hydrogen process, the GHG emissions are 12.8 kg CO<sub>2e</sub> per kg hydrogen, an increase of 36% from fossil-fuel hydrogen. Similar to the methanol cases, alternate process configurations and less use of fossil energy could lower GHG emissions.

The GHG emissions for the MSW-hydrogen process are 15.6 kg CO<sub>2e</sub> per kg hydrogen, an increase of about 67% over fossil-fuel hydrogen. This increase can be attributed to the low hydrogen content in the MSW feed. As shown in Table 2, MSW contains half the hydrogen content of MPW. This leads to a lower hydrogen yield from the MSW-hydrogen process, thereby increasing the GHG emissions per kg of hydrogen. If credit is assigned to the MSW-hydrogen process for the avoidance of methane emissions at the landfill (1.6 kg CO<sub>2</sub> avoided per kg MSW),<sup>64</sup> the overall GHG emissions drop to 2.6 kg CO<sub>2e</sub> per kg hydrogen, a reduction of 73% from fossil-fuel derived hydrogen. The CO<sub>2</sub> credit is calculated only based on the amount of

MSW that is gasified (any solid residue from the gasification process is not included).

### Life cycle assessment

While MFI provides GHG emissions and energy consumption within the current United States supply chain, LCA offers a more holistic overview of global environmental impacts. To that end, an LCA was conducted for both the MPW-methanol and MPW-hydrogen processes. We used the Tool for the Reduction and Assessment of Chemicals and Other Environmental Impacts (TRACI 2.1, US 2008) and Available WAtER REMaining (AWARE) methods and ecoinvent version 3.3 background data (U.S.-specific when available, global otherwise) in SimaPro LCA software to calculate the acidification, carcinogenics, ecotoxicity, eutrophication, fossil fuel depletion, non-carcinogenics, ozone depletion, respiratory effects, smog, and water use impacts of gasification of mixed plastic waste (Fig. 8). The process was assessed using a cradle-to-gate approach, from MPW curbside collection to the final gasification product; impacts associated with manufacturing the original plastic feedstock or utilizing the produced chemicals were not included. Credits were given for co-products. Standard deviations were estimated using ecoinvent log-normal uncertainty distributions and Monte Carlo analysis with 1000 iterations.





**Fig. 8** Life cycle assessment results for MPW-methanol and MPW-hydrogen. (A) Comparison of life cycle impacts for MPW-methanol and fossil-fuel methanol. (B) Contribution of process components to the MPW-methanol process. (C) Comparison of life cycle impacts for MPW-hydrogen and fossil-fuel hydrogen. (D) Contribution of process components to the MPW-hydrogen process. Calculations were conducted with TRACI 2.1 US 2008 and AWARE methods, SimaPro software, and ecoinvent 3.3 background data. The detailed results are given in Table S20.†

**Methanol.** The MPW-methanol case is predicted to exhibit lower impacts than fossil-fuel-derived methanol for acidification (statistically significant), fossil fuel depletion (statistically significant), non-carcinogenics, ozone depletion, and smog (statistically significant), while carcinogenics, ecotoxicity, eutrophication, particulates formation (statistically significant), and water use (statistically significant) are higher (Fig. 8A). The lower impact categories are primarily due to avoided emissions from the co-generation of steam (Fig. 8B). Only acidification, fossil fuel depletion, and smog remain below fossil-fuel-derived methanol levels without these co-product credits. Most of the impact categories are dominated by natural gas for the gasification reactors (4–79% of all metrics except water use), collection and sorting of the MPW feedstock (8–45%), and electricity (10–69%). Cooling and boiler feed water combined account for 99% of water use, which is an order of magnitude higher than virgin methanol since all cooling requirements in the gasification plant were met by cooling water. Commercial plants would likely instead use a combination of fin-fan coolers and cooling water.

Catalysts, infrastructure, and disposal of waste ash, and waste-water have relatively minimal impacts, although it should be noted that the olivine bed material, ZnO bed, and steam methane reforming catalysts all contain critical materials according to the U.S. Geological Survey (Mg, Zn, and Ni, respectively).<sup>69</sup> For each catalyst, we assumed a 5-year catalyst lifetime.<sup>45,46</sup>

**Hydrogen.** The MPW-hydrogen case exhibits lower impacts than traditional hydrogen production in the carcinogenics, eutrophication, fossil fuel depletion, particulates, and smog categories; these results are statistically significant excepting carcinogenics. Acidification, ecotoxicity, non-carcinogenics, ozone depletion, and water use are higher than fossil-fuel-derived hydrogen, although these differences fall within estimated uncertainty ranges (Fig. 8C). Without co-product credits from the generated electricity and steam, only smog remains lower for gasification than for conventional hydrogen. Natural gas for the gasification reactors and MPW feedstock preparation account for 12–90% and 8–79%, respectively, of all metrics except water use (Fig. 8D). Catalysts have a larger





impact in this case than for methanol – contributing 7–22% to carcinogenics, ecotoxicity, eutrophication, and non-carcinogenics – which is due to the higher quantity of olivine bed material used per unit of product generated.

LCA combined with MFI suggests that while gasification may not reduce GHG emissions for the process configurations described in this study, it can be a promising approach to minimize environmental impacts in several other natural environment, human health, and resource consumption categories. Nevertheless, environmental impacts across all assessed categories could be minimized if natural gas and electricity requirements were reduced, either through technological improvements to the gasification or utilization of more renewable electricity and heat sources. Avoided emissions also play a crucial role in lowering the environmental impacts of gasification, particularly in the MPW-hydrogen case, highlighting the importance of efficiently capturing and utilizing all co-products. It should be noted that gasification global warming potentials calculated by LCA (0.7 kg CO<sub>2</sub>e per kg methanol and 10.8 kg CO<sub>2</sub>e per kg hydrogen, Table S20†) are slightly lower than those from MFI primarily because the steam and electricity co-products are estimated to be more impactful in the ecoinvent database and therefore supply more negative credits. Fossil fuel depletion cannot be directly compared to MFI supply chain energy use as the former includes weighting factors associated with the potential of a given fuel to become more difficult to extract in the future.

## Discussion

### Reactor design for MPW gasification

The experimental data<sup>32</sup> used to model the MPW gasifier was based on a pilot plant trial that used a dual fluidized bed design and we have retained the same design for our analysis. However, there are several other gasifier designs that have been used for waste gasification. For example, the ‘Carbon Renewal Technology’ from Eastman Chemicals uses an entrained flow gasifier for waste plastics recycling. The company completed several trials and announced the technology in 2019.<sup>70</sup> Gidara Energy uses a high-temperature Winkler gasifier to convert biomass per MSW to syngas and produces methanol.<sup>71</sup> Enerkem uses a bubbling fluidized bed gasifier to gasify biomass per MSW and the final product is methanol.<sup>19</sup> Though we have considered a specific design, namely a dual fluidized bed system, the insights obtained here likely would apply broadly to gasification processes as long as the input oxidant ratios, operating conditions, and syngas quality are in the same range. Furthermore, we varied parameters such as capital costs and syngas quality in the sensitivity analysis to account for such uncertainties due to gasifier design and other process changes for such newer processes.

### Methanol synthesis cases

Our TEA results show that at the base case conditions considered, MPW and MSW gasification may not be able to

produce methanol at prices that are competitive with current market prices. However, significant opportunities exist to reduce the MSP of these pathways.

Methanol produced from natural gas has an average market price of \$0.30 kg<sup>-1</sup>. Our analysis indicates that for a plant size of 240 MT per D, MPW and MSW gasification would be able to produce methanol at MSPs of \$0.70 kg<sup>-1</sup> and \$0.55 kg<sup>-1</sup>, respectively. Although the MSP of MPW-methanol is higher, there is potential to approach cost parity with the market methanol price (\$0.30 kg<sup>-1</sup>) if the plastic feedstock is available at \$0.02 kg<sup>-1</sup>, as shown in Fig. 9. Some waste polyolefin streams that do not have a recycling market, like films and flexibles are potentially available at this low cost. ‘C grade film’ which consists of low-density polyethylene (LDPE), linear low-density polyethylene (LLDPE), HDPE, or PP films has a cost of \$0–\$0.02 kg<sup>-1</sup>.<sup>38</sup> Furthermore, the chemical compositions of these streams are quite similar to the PE and PP composition used in the base case.<sup>72</sup> Hence, if these types of streams can provide a high syngas yield of 1.4 kg syngas per kg solid plastic, this opens an opportunity for methanol production by MPW steam gasification at a competitive price.

The CAPEX contributes ~23% to the methanol MSP from the MPW-methanol process. Due to the inherent chemistry of the gasification reactions in the gasifier that produces methane and tar, the reforming and syngas preparation in MPW gasification comprise a gasifier, tar reformer, and steam reformer distributed across the first two process sections, namely gasification and syngas preparation. In comparison, a natural gas-based methanol plant only has a one-step reforming in a steam reformer for syngas production. This results in a higher contribution of capital costs to the MSP in the MPW-methanol pathway. Small-capacity, US-based methanol plants using natural gas as the feed have CAPEX costs of about \$247k per MT per D.<sup>73</sup> Using this estimate for the current plant size of 353 MT per D methanol, the capital investment for a natural gas-based methanol plant will be around \$87M. Hence, the TCI for a methanol plant operating on MPW feedstock could



Fig. 9 Methanol MSP for varied MPW feedstock prices. Cost parity with fossil-fuel-based methanol (\$0.30 kg<sup>-1</sup>) could be achieved if MPW feedstock is available for ≤\$0.02 kg<sup>-1</sup>.



be more expensive than a conventional natural gas-based facility by  $\geq 70\%$ .

Comparing the MPW and MSW feedstock MSP breakdowns in Fig. 10, it can be observed that changing the feedstock cost from  $\$0.60 \text{ kg}^{-1}$  in the MPW scenario to  $\$0 \text{ kg}^{-1}$  in the MSW scenario is overshadowed by a simultaneous increase in capital costs and other operational costs (largely driven by changes in feedstock composition and the effect on syngas yield). As shown in Table 3, the product mass yield for the MSW-methanol process is much lower at 0.48 kg methanol per kg MSW than the 1.47 kg methanol per kg in the MPW-methanol process. Hence, even though the MSW feedstock price is assumed to be zero, the MSP is still high for the MSW-methanol process at  $\$0.55 \text{ kg}^{-1}$ . This MSP is primarily driven by the lower syngas yield for MSW gasification. Hence, the high syngas yield of waste plastics is a desirable feature for solid feedstocks. An effective strategy to bring down the MSP remains in finding waste plastic streams with low cost that can provide high syngas yield (1.4 kg syngas per kg MPW). Furthermore, for processes like methanol and hydrogen, a high molar H/C ratio ( $\geq 2$ ) in the chemical composition of the feedstock is desirable since this affects the  $\text{H}_2/\text{CO}$  ratio in the syngas from the stoichiometry of reactions. Natural gas has an H/C ratio of 4 and is the primary feedstock to produce methanol and hydrogen. Plastics like PP ( $\text{C}_3\text{H}_6$ )<sub>n</sub> and PE ( $\text{C}_2\text{H}_4$ )<sub>n</sub> have H/C ratios of 2. However, other plastics like poly(ethylene tere-

phthalate) ( $\text{C}_{10}\text{H}_8\text{O}_4$ )<sub>n</sub> or polyvinyl chloride ( $\text{C}_2\text{H}_3\text{Cl}$ )<sub>n</sub> have lower H/C ratios and will produce poor syngas yields. Hence, the chemical makeup of the final product of gasification should be considered while studying the potential of different plastic types for gasification.

In the MSW-methanol process, the MSP is affected most by plant size and the tipping fee. Both these factors are geography-dependent, and locations with large MSW availability and high tipping fees will help make the process economics favorable. The tornado plot for sensitivity analysis on MSW-methanol is included in Fig. S4.†

### Hydrogen cases

The base case process simulation of the MPW-hydrogen process results in a hydrogen yield of 29.1 g  $\text{H}_2$  per 100 g MPW. This is 68% of the stoichiometric maximum (42.9 g  $\text{H}_2$  per 100 g MPW). The corresponding MSP of hydrogen from MPW gasification is  $\$3.41 \text{ kg}^{-1}$ , almost three times the market price for fossil-fuel-derived hydrogen ( $\$1.15 \text{ kg}^{-1}$ ). The large difference between the prices of these pathways can be partly explained based on the chemistry of the reaction pathways to hydrogen.

Steam reforming of natural gas to produce hydrogen:



Plastic waste steam gasification pathway:



From the stoichiometry of these reactions, the hydrogen yield per carbon atom is 4 in the natural gas pathway and 3 for plastic waste gasification due to their inherent chemical compositions. Furthermore, the feedstock costs are different; natural gas is available for  $\$0.15 \text{ kg}^{-1}$  and the waste plastics price is taken as  $\$0.60 \text{ kg}^{-1}$  in this study.

For hydrogen, the market price benchmark is  $\$1.15 \text{ kg}^{-1}$ , whereas our analysis estimates that the MPW-hydrogen process exhibits an MSP of  $\$3.41 \text{ kg}^{-1}$ . Recent industry reports for the waste plastic-to-hydrogen pathway targeted a hydrogen sales price of  $\$3.50 \text{ kg}^{-1}$ ,<sup>74</sup> which is similar to the estimation by our model. Most of the key TEA takeaways for the hydrogen pathway remain the same as for the methanol pathways. The MSP for hydrogen from the MPW-hydrogen pathway approaches the fossil-fuel hydrogen price if the waste plastic feedstock price is zero. The PSA hydrogen recovery is an important variable for both MSW- and MPW-based processes because hydrogen lost in the off-gases is combusted as fuel and negatively impacts process economics.

In the MSW-hydrogen model, the base case predicts a mass yield of 9.4 g per 100 g MSW. This low yield can be attributed to the initial low hydrogen content of 6.9% in MSW, as shown in Table 2. A recent industry estimate for the waste-to-hydrogen pathway predicts a yield of 6.5 g per 100 g of waste for an upcoming plant.<sup>75</sup> Previous investigations on the MSW-hydrogen pathway report yields as low as 6.1 g  $\text{H}_2$  per 100 g MSW<sup>76</sup> and as high as 12.6 g  $\text{H}_2$  per 100 g MSW<sup>77</sup> for the best-case



**Fig. 10** Comparison of MSP breakdown of methanol obtained from MPW and MSW gasification. Comparing MPW and MSW, the large reduction of feedstock contribution to MSP in MSW is accompanied by a simultaneous increase in the capital cost and other operational costs (fixed cost) due to the lower product yield of the MSW-methanol process.



scenario, which considers complete WGS conversion of all carbonaceous compounds resulting in higher yield.

The MSP for the MSW-hydrogen pathway was estimated to be \$3.24 kg<sup>-1</sup>. Plant capacity has the largest impact of all variables studied on the hydrogen MSP for the MSW-gasification route. Ng and Phan conducted a TEA of a waste-to-hydrogen process<sup>78</sup> and reported that larger plant capacities are desirable for process economics. They also reported hydrogen MSP prices of \$2.95 kg<sup>-1</sup> and \$8.17 kg<sup>-1</sup> for plant sizes of 2400 MT per D and 48 MT per D, respectively. Some industry experts estimate that for MSW-to-H<sub>2</sub> technology, the hydrogen MSP at \$5 kg<sup>-1</sup> will go down to \$3 kg<sup>-1</sup> by 2025.<sup>79</sup> In comparison, a proton-exchange-membrane-based grid-connected electrolysis<sup>80</sup> can produce green H<sub>2</sub> at \$5.5 kg<sup>-1</sup> at 61% system efficiency and 7 ' kW h electricity cost. The recent Global Hydrogen Review Report 2021<sup>30</sup> estimates that green H<sub>2</sub> costs from different pathways lie in the range of \$3–\$8 kg<sup>-1</sup> based on local renewable electricity costs for different pathways (onshore/offshore wind, solar photovoltaics).

### Co-product credit

The MPW-methanol process has an export stream of low-pressure steam (3 bar) with a flow rate of 1584 MT per D, as shown in Fig. S11.† This is a large stream considering the methanol production of 354 MT per D. The large steam generation is due to the availability of many high-temperature streams in the process in the range of 565 °C–890 °C. There are three heat recovery steam generators (HRSGs) in the MPW-methanol process that produce medium pressure steam (45 bar). In a natural gas-based plant, there is only one HRSG since reforming at ~850 °C is performed only once, unlike in the MPW-methanol process, where multiple reactors are needed to convert the MPW fully to syngas. This results in added costs and higher GHG emissions for the MPW-methanol process.

Conversely, the co-product credit benefits most sustainability metrics due to avoided emissions from steam generation. Similarly, the MPW-hydrogen exhibits an electricity export in addition to steam export. The WGS reactor operates at 20 bar, unlike the methanol synthesis reactor, which operates at 80 bar. The electricity generation from the steam turbine exceeds the demand of the MPW-hydrogen process, resulting in a net electricity export of 2.8 MW for the 240 MT per D MPW-hydrogen process.

### Integration with existing facilities

An opportunity for future research could be the integration of the MPW and MSW gasification pathways with existing facilities. As shown in Fig. S12,† the gasification pathways differ from conventional natural gas-based processes only in the upstream part of the plant. After syngas generation, the processes remain identical, which provides an opportunity for integration with existing methanol and hydrogen plants. For instance, the CAPEX of the methanol synthesis section contributed almost half of the CAPEX of the MPW-methanol plant, as shown in Fig. 2A. If the syngas produced by MPW-gasification

can be routed to an existing methanol plant for compression and synthesis, it would increase methanol production of the existing plant and reduce CAPEX costs for the MPW-methanol plant. The scale of the methanol plant, 353 MT per D, considered in the base case here is small compared to conventional natural gas-based methanol plants which are in the range of 2000–3000 MT per D capacity.<sup>61</sup> Thus, existing design margins could perhaps accommodate the additional syngas from an MPW-gasification plant in existing facilities without much need for revamping or debottlenecking. This proposition, however, would need to be assessed carefully to ascertain technical feasibility. Nevertheless, integration with existing facilities is an important area of research for MPW and MSW gasification technologies.

### Sustainability implications

The GHG emissions of the MPW-gasification processes using the process configurations described in this study are higher than their fossil-fuel counterparts, as shown in Fig. 7. The increase can be attributed to the change in feedstock from natural gas to MPW, which requires additional endothermic reforming steps after gasification, resulting in higher GHG emissions from fossil energy use. Furthermore, primarily due to the co-product credits of the MPW-gasification processes, both the MPW-methanol and MPW-hydrogen cases exhibit acidification, carcinogenic and non-carcinogenic impacts on human health, ecotoxicity, eutrophication, fossil fuel depletion, ozone formation, and smog formation lower than or statistically equivalent to their fossil-derived equivalents. Overall, gasification of plastics must seek to reduce natural gas and electricity requirements through alternative process configurations, as well as to reduce feedstock transportation distances, in order to minimize environmental impacts across all assessed categories.

## Conclusions

This work investigates the economic potential and possible opportunities for gasification pathways of MPW to produce methanol and hydrogen. Based on the assumptions in this study, methanol and hydrogen produced by MPW gasification have MSPs of \$0.70 kg<sup>-1</sup> and \$3.41 kg<sup>-1</sup>, respectively. Though the processes at base case conditions have higher MSPs than their fossil-fuel counterparts, significant opportunities exist to reduce the MSPs of methanol and hydrogen by the MPW gasification pathway. The process economics in MPW-based pathways are mainly affected by the syngas yield and the cost of waste plastic feedstock. Our supply chain energy analysis by the MFI tool shows that the supply chain energy requirements for both the methanol and hydrogen pathways are reduced by 52% and 56%, respectively, compared to their fossil-fuel counterparts. However, the GHG emissions are higher by 166% for methanol and 36% for hydrogen. Therefore, using the MPW gasification pathway to produce methanol and hydrogen in this study by the processes described here results



in a net increase in GHG emissions. The LCA analysis shows that MPW-gasification pathways have lower smog formation, acidification, non-carcinogenic impacts on human health, ozone depletion, eutrophication and particulates than their fossil-fuel counterparts, primarily due to co-product credits from steam and electricity export. Overall, this work provides valuable information on the relative impact of different parameters on the process economics of MPW gasification pathways. This can help guide future research toward optimizing the variables that have the greatest impact on bringing down the MSP of products from MPW gasification. Although this work is focused on the final products of methanol and hydrogen, the key takeaways from the economic analysis will apply broadly to gasification processes utilizing waste plastic feedstocks.

## Conflicts of interest

None to declare.

## Acknowledgements

This work was authored in part by Alliance for Sustainable Energy, LLC, the manager, and operator of the National Renewable Energy Laboratory for the U.S. Department of Energy (DOE) under contract no. DE-AC36-08GO28308. Funding was provided by the US Department of Energy, Office of Energy Efficiency and Renewable Energy, Advanced Materials and Manufacturing Technologies Office (AMO) and Bioenergy Technologies Office (BETO). This work was performed as part of the Bio-Optimized Technologies to keep Thermoplastics out of Landfills and the Environment (BOTTLE) Consortium and was supported by AMO and BETO under contract no. DE-AC36-08GO28308 with the National Renewable Energy Laboratory (NREL), operated by Alliance for Sustainable Energy, LLC. The views expressed in the article do not necessarily represent the views of the DOE or the U.S. Government. The U.S. Government retains and the publisher, by accepting the article for publication, acknowledges that the U.S. Government retains a nonexclusive, paid-up, irrevocable, worldwide license to publish or reproduce the published form of this work, or allow others to do so, for U.S. Government purposes.

## References

- 1 M. Hong and E. Y.-X. Chen, *Green Chem.*, 2017, **19**, 3692–3706.
- 2 A. Rahimi and J. M. García, *Nat. Rev. Chem.*, 2017, **1**, 1–11.
- 3 K. Ragaert, L. Delva and K. Van Geem, *Waste Manage.*, 2017, **69**, 24–58.
- 4 SRIC Report - PEP Report 199E - Advances in Mixed Plastics Chemical Recycling|IHS Markit, <https://ihsmarkit.com/products/pep-199e-advances-in-mixed-plastics-chemical-recycling.html>, (accessed December 14, 2021).
- 5 G. W. Coates and Y. D. Y. L. Getzler, *Nat. Rev. Mater.*, 2020, **5**, 501–516.
- 6 I. Vollmer, M. J. F. Jenks, M. C. P. Roelands, R. J. White, T. van Harmelen, P. de Wild, G. P. van der Laan, F. Meirer, J. T. F. Keurentjes and B. M. Weckhuysen, *Angew. Chem., Int. Ed.*, 2020, **59**, 15402–15423.
- 7 Waste Plastic Chemical Recycling via Pyrolysis|IHS Markit, <https://ihsmarkit.com/info/0921/wasteplasticchemicalrecycling.html>, (accessed December 14, 2021).
- 8 O. Dogu, M. Pelucchi, R. Van de Vijver, P. H. M. Van Steenberge, D. R. D'hooge, A. Cuoci, M. Mehl, A. Frassoldati, T. Faravelli and K. M. Van Geem, *Prog. Energy Combust. Sci.*, 2021, **84**, 100901.
- 9 L. D. Ellis, N. A. Rorrer, K. P. Sullivan, M. Otto, J. E. McGeehan, Y. Román-Leshkov, N. Wierckx and G. T. Beckham, *Nat. Catal.*, 2021, **4**, 539–556.
- 10 S. C. Kosloski-Oh, Z. A. Wood, Y. Manjarrez, J. P. de los Rios and M. E. Fieser, *Mater. Horiz.*, 2021, **8**, 1084–1129.
- 11 A. J. Martin, C. Mondelli, S. D. Jaydev and J. Pérez-Ramírez, *Chem*, 2021, **7**, 1487–1533.
- 12 C. Shi, L. T. Reilly, V. S. Phani Kumar, M. W. Coile, S. R. Nicholson, L. J. Broadbelt, G. T. Beckham and E. Y.-X. Chen, *Chem*, 2021, **7**, 2896–2912.
- 13 5.1. Gasification Introduction|netl.doe.gov, <https://netl.doe.gov/research/Coal/energy-systems/gasification/gasifiedia/intro-to-gasification>, (accessed December 10, 2021).
- 14 J. Rostrup-nielsen and L. J. Christiansen, in *Concepts In Syngas Manufacture*, Imperial College Press, 1st edn, 2011, vol. 10, pp. 3–138.
- 15 G. C. Young, in *Municipal Solid Waste to Energy Conversion Processes: Economic, Technical, and Renewable Comparisons*, John Wiley & Sons, Inc., 2010, pp. 1–15.
- 16 P. J. Reddy, *Energy Recovery from Municipal Solid Waste by Thermal Conversion Technologies*, CRC Press, 2016.
- 17 Waste-to-Energy from Municipal Solid Wastes, <https://www.energy.gov/sites/prod/files/2019/08/f66/BETO-Waste-to-Energy-Report-August-2019.pdf>.
- 18 C. Mukherjee, J. Denney, E. G. Mbonimpa, J. Slagley and R. Bhowmik, *Renewable Sustainable Energy Rev.*, 2020, **119**, 109512.
- 19 Carbon Recycling|Advanced Thermochemical Process|Enerkem, <https://enerkem.com/process-technology/carbon-recycling/>, (accessed September 19, 2021).
- 20 G. Lopez, M. Artetxe, M. Amutio, J. Alvarez, J. Bilbao and M. Olazar, *Renewable Sustainable Energy Rev.*, 2018, **82**, 576–596.
- 21 M. Fisher, *Air-Blown Versus Oxygen Blown Gasification*, British Coal Corporation, Coal Technology Development Division, Clean Coal Power Generation Group, 1996.
- 22 C. D. Chapman, R. J. Taylor and A. Faraz, *Proc. Inst. Civ. Eng.: Waste Resour. Manage.*, 2014, **167**, 15–24.
- 23 A. Midilli, H. Kucuk, M. Haciosmanoglu, U. Akbulut and I. Dincer, *Int. J. Energy Res.*, 2022, **46**, 4001–4032.
- 24 S.-W. Wang, D.-X. Li, W.-B. Ruan, C.-L. Jin and M. R. Farahani, *Energy Sources, Part B*, 2018, **13**, 351–356.





- 25 H. Almohamadi, *AIMS Energy*, 2020, **9**, 50–67.
- 26 J. Goyal, *Advances in Mixed Plastics Chemical Recycling*, PEP Report 199E, 2020.
- 27 S. R. Nicholson, J. E. Rorrer, A. Singh, M. O. Konev, N. A. Rorrer, A. C. Carpenter, A. J. Jacobsen, Y. Román-Leshkov and G. T. Beckham, *Annu. Rev. Chem. Biomol. Eng.*, 2022, **13**, 301–324.
- 28 The Methanol Industry|Methanol Institute| <https://www.methanol.org>, <https://www.methanol.org/the-methanol-industry/>, (accessed December 23, 2021).
- 29 *The Future of Hydrogen – Analysis – IEA*, 2019.
- 30 International Energy Agency, *Global Hydrogen Review 2021*, OECD, 2021.
- 31 D. Proctor, Waste-to-Hydrogen Project Set for California, <https://www.powermag.com/waste-to-hydrogen-project-set-for-california/>, (accessed September 19, 2021).
- 32 V. Wilk and H. Hofbauer, *Fuel*, 2013, **107**, 787–799.
- 33 E. Chornet, B. Valsecchi, G. Drolet, M. Gagnon and B. Nguyen, *US Pat*, US20100051875A1, 2010.
- 34 Companies are placing big bets on plastics recycling. Are the odds in their favor?, <https://cen.acs.org/environment/sustainability/Companies-placing-big-bets-plastics/98/i39>, (accessed December 13, 2021).
- 35 A. Milbrandt, K. Coney, A. Badgett and G. T. Beckham, *Resour., Conserv. Recycl.*, 2022, **183**, 106363.
- 36 D. Saebea, P. Ruengrit, A. Arpornwicheanop and Y. Patcharavorachot, *Energy Rep.*, 2020, **6**, 202–207.
- 37 A. M. Ward, A. J. M. Oprins and R. Narayanaswamy, *US Pat*, US10233395B2, 2019.
- 38 Recycling Markets, <https://www.recyclingmarkets.net/>, (accessed September 19, 2021).
- 39 C. Valkenburg, C. W. Walton, B. L. Thompson, M. A. Gerber, S. B. Jones and D. J. Stevens, *Municipal Solid Waste (MSW) to Liquid Fuels Synthesis, Volume 1: Availability of Feedstock and Technology*, 2008.
- 40 J. Haydari, Modelling of Gasification of Refuse-derived fuel (RDF) based on laboratory experiments, [https://uest.ntua.gr/cyprus2016/proceedings/pdf/Haydari\\_modelling\\_gasification.pdf](https://uest.ntua.gr/cyprus2016/proceedings/pdf/Haydari_modelling_gasification.pdf).
- 41 J. Paszkowski, M. Domański, J. Caban, J. Zarajczyk, M. Pristavka and P. Findura, *Agric. Eng.*, 2020, **24**, 83–90.
- 42 M. Hu, D. Guo, C. Ma, Z. Hu, B. Zhang, B. Xiao, S. Luo and J. Wang, *Energy*, 2015, **90**, 857–863.
- 43 S. Boxman and B. F. Staley, *Analysis of MSW Landfill Tipping Fees – 2020*, Environment Research & Education Foundation (2021), 2021.
- 44 Polyethylene – Low Density (LDPE), granule, 5 mm nominal granule size, weight 200 g|Sigma-Aldrich, <https://www.sigmaaldrich.com/>, (accessed January 3, 2022).
- 45 S. Phillips, A. Aden, J. Jechura, D. Dayton and T. Eggeman, *Thermochemical Ethanol via Indirect Gasification and Mixed Alcohol Synthesis of Lignocellulosic Biomass*, NREL/TP-510-41168, 2007.
- 46 P. Spath, A. Aden, T. Eggeman, M. Ringer, B. Wallace and J. Jechura, *Biomass to Hydrogen Production Detailed Design and Economics Utilizing the Battelle Columbus Laboratory Indirectly-Heated Gasifier*, NREL, 2005.
- 47 *Methanol: The Basic Chemical and Energy Feedstock of the Future*, ed. M. Bertau, H. Offermanns, L. Plass, F. Schmidt and H.-J. Wernicke, Springer Berlin Heidelberg, Berlin, Heidelberg, 2014.
- 48 Methanol Plants – Chemical Industry, <https://www.thyssenkrupp-industrial-solutions.com/en/products-and-services/chemical-plants-and-processes/methanol-plants/adwinmethanol>, (accessed January 3, 2022).
- 49 LO-CAT®|Sulfur Recovery Solution|Merichem, <https://www.merichem.com/technology/sulfur-recovery-with-lo-cat/>, (accessed December 8, 2021).
- 50 S. Lee, in *Methanol Synthesis Technology*, CRC Press, Boca Raton, Florida, 1st edn, 1990, p. 33.
- 51 A. Dutta and S. D. Phillips, *Thermochemical Ethanol via Direct Gasification and Mixed Alcohol Synthesis of Lignocellulosic Biomass*, 2009.
- 52 M.-H. Labrie, Waste-to-methanol: a commercial reality with Enkern, <https://www.methanol.org/wp-content/uploads/2016/07/Marie-H%C3%A9l%C3%A8ne-Labrie.pdf>.
- 53 G. Energy, GIDARA Energy's Advanced Methanol Rotterdam will convert non-recyclable waste into advanced biofuels, <https://www.prnewswire.com/news-releases/gidara-energys-advanced-methanol-rotterdam-will-convert-non-recyclable-waste-into-advanced-biofuels-301528698.html>, (accessed April 22, 2022).
- 54 W. A. Amos, *Biological Water-Gas Shift Conversion of Carbon Monoxide to Hydrogen: Milestone Completion Report*, 2004.
- 55 R. A. Meyers, in *Handbook of Petroleum Refining Processes, Third Edition*, McGraw-Hill Education, New York, 3rd edn, 2004.
- 56 S. Czernik and R. J. French, *Energy Fuels*, 2006, **20**, 754–758.
- 57 G. Lopez, A. Erkiaga, M. Artetxe, M. Amutio, J. Bilbao and M. Olazar, *Ind. Eng. Chem. Res.*, 2015, **54**, 9536–9544.
- 58 *2012 Gas Processes Handbook – Hydrogen (UOP PSA)*, Hydrocarbon Processing, Gulf Publishing Company, 2012.
- 59 NREL, Materials Flows through Industry (MFI), Materials Flows through Industry (MFI).
- 60 Franklin Associates, *Life cycle impacts for postconsumer recycled resins: PET, HDPE and PP*, 2018.
- 61 A. Frei and R. A. Meyers, in *Handbook of Petrochemicals Production Processes*, McGraw-Hill, 1st edn, 2005, vol. 1, pp. 7.3–7.17.
- 62 V. M. Ehlinger, K. J. Gabriel, M. M. B. Noureldin and M. M. El-Halwagi, *ACS Sustainable Chem. Eng.*, 2014, **2**, 30–37.
- 63 M. M. B. Noureldin, N. O. Elbashir and M. M. El-Halwagi, *Ind. Eng. Chem. Res.*, 2014, **53**, 1841–1855.
- 64 N. Patel, *Municipal Solid Waste and its Role in Sustainability*, IEA Bioenergy, United Kingdom, 2003.
- 65 O. US EPA, Greenhouse Gas Equivalencies Calculator, <https://www.epa.gov/energy/greenhouse-gas-equivalencies-calculator>, (accessed December 28, 2022).



- 66 B. Bahor, M. Van Brunt, K. Weitz and A. Szurgot, *J. Environ. Eng.*, 2010, **136**, 749–755.
- 67 U. Lee, J. Han and M. Wang, *J. Cleaner Prod.*, 2017, **166**, 335–342.
- 68 S.-J. Royer, S. Ferrón, S. T. Wilson and D. M. Karl, *PLoS One*, 2018, **13**, e0200574.
- 69 U.S. Geological Survey Releases 2022 List of Critical Minerals|U.S. Geological Survey, <https://www.usgs.gov/news/national-news-release/us-geological-survey-releases-2022-list-critical-minerals>, (accessed April 26, 2022).
- 70 B. Coleman, R. Waymire, N. Brown and C. J. Pierce, LCA carbon footprint summary report for Eastman carbon renewal technology, <https://www.eastman.com/Company/Circular-Economy/Resources/Documents/CRT-Technical-LCA-report.pdf>, (accessed May 22, 2023).
- 71 Advanced Methanol Amsterdam, <https://www.gidara-energy.com/advanced-methanol-amsterdam>, (accessed May 20, 2023).
- 72 L. Bedard, T. Matta, L. Thompson, S. Dearman, S. Mouw and A. Tanimoto, *Addressing the Challenge of Film and Flexible Packaging Data, The Recycling Partnership*, The Recycling Partnership, 2021.
- 73 Small-scale methanol technologies offer flexibility, cost effectiveness, <https://www.gasprocessingnews.com/features/201510/small-scale-methanol-technologies-offer-flexibility-cost-effectiveness.aspx>, (accessed September 18, 2021).
- 74 Linde, Hydrogen Utopia to deploy plastic waste-to-hydrogen technology in Poland|S&P Global Platts, <https://www.spglobal.com/platts/en/market-insights/latest-news/electric-power/090621-linde-hydrogen-utopia-to-deploy-plastic-waste-to-hydrogen-technology-in-poland>, (accessed December 14, 2021).
- 75 R. S. Inc, Raven SR to build a waste-to-hydrogen project in Aragón, Spain, <https://www.prnewswire.com/news-releases/raven-sr-to-build-a-waste-to-hydrogen-project-in-aragon-spain-301513169.html>, (accessed March 29, 2022).
- 76 A. D. Pasternak, J. H. Richardson, R. S. Rogers, C. B. Thorsness, H. Wallman, G. N. Richter and J. K. Wolfenbarger, *MSW to hydrogen*, United States, 1994.
- 77 M. He, Z. Hu, B. Xiao, J. Li, X. Guo, S. Luo, F. Yang, Y. Feng, G. Yang and S. Liu, *Int. J. Hydrogen Energy*, 2009, **34**, 195–203.
- 78 K. S. Ng and A. N. Phan, *Resour., Conserv. Recycl.*, 2021, **167**, 105392.
- 79 L. Collins, (l\_collins), “It’s much cheaper to produce green hydrogen from waste than renewables”|Recharge, <https://www.rechargenews.com/transition/its-much-cheaper-to-produce-green-hydrogen-from-waste-than-renewables/2-1-801160>, (accessed December 9, 2021).
- 80 M. R. Shaner, H. A. Atwater, N. S. Lewis and E. W. McFarland, *Energy Environ. Sci.*, 2016, **9**, 2354–2371.

